

1 A process-based framework for 2 quantifying sampling completeness of 3 species interaction networks

4 Michael D. Catchen^{1,3,2}, Timothée Poisot^{2,3}, Laura J. Pollock^{1,3}, Andrew Gonzalez^{1,3}

5 Corresponding Author: michael.catchen@umontreal.ca

6 ¹McGill University, Department of Biology, Québec, Canada

7 ²Université de Montréal, Québec, Canada

8 ³Québec Centre for Biodiversity Science, Québec, Canada

9 **Abstract**

10 Species interaction networks underpin ecosystem function and persistence, but their study is
11 hindered by lack of empirical knowledge about interactions. Many interactions occur in nature that
12 have not been observed or recorded. We develop a process-based framework for simulating species
13 interaction accumulation curves that accounts for spatiotemporal variation species interaction
14 networks. We do this by explicitly linking interaction realization and detection rates to species
15 abundance. We implement this framework in a software package, SpeciesInteractionSamplers.jl,
16 which enables researchers to evaluate monitoring strategies and assess the completeness of
17 empirical interaction datasets under biologically realistic assumptions. Together, this framework and
18 software provide a foundation for quantifying the Eltonian shortfall, and for improving the design of
19 interaction monitoring networks.

20 **1 Introduction**

21 Species interactions — like predation, pollination, and parasitism — govern the flow of biomass and
22 energy through ecosystems, ultimately enabling persistence of biodiversity and ecosystem
23 functioning. Despite their importance for ecosystem processes, species interactions are a major
24 knowledge gap in knowledge of life on Earth; the so-called “Eltonian shortfall” ([Hortal et al. 2015](#)).
25 Better monitoring of species interactions is an imperative to understand and predict the impacts of
26 anthropogenic change on biodiversity ([Makiola et al. 2020](#)), ecosystem function ([Bartley et al. 2019](#)),
27 and to anticipate disease spillover to prevent future pandemics ([Carlson et al. 2022](#), [Becker et al.](#)

28 2022). We lack sufficient data to meet these challenges (Poisot et al. 2021) because species
29 interactions are difficult to sample (Jordano 2016a; b). Many, if not most, species interactions that
30 occur in nature have not yet been detected and recorded (Cirtwill et al. 2019). We can be confident
31 two species can feasibly interact if we have a record of it (assuming each species was correctly
32 identified), but unsure that two species could not feasibly interact if we have never observed it, let
33 alone if we have few (or zero) records of these species co-occurring. Consequently, empirically
34 constructed interaction networks contain many false negatives, where two species interact, but we
35 lack any record of it.

36 Recent work has aimed to address this data gap by using species-level information (e.g. traits,
37 abundance, range, phylogenies, etc.) to predict interaction feasibility (Terry and Lewis 2020, Caron et
38 al. 2022), and for spatially and temporally explicit prediction of species interaction networks
39 (Strydom et al. 2021). One challenge here is that we don't have a good idea how many feasible
40 interactions are "missing" from these networks, as species interactions vary in how often they are
41 realized and their intrinsic detectability (Cirtwill et al. 2019). Here, we develop a spatiotemporally
42 explicit process-based framework for modeling stochastic interaction realization and imperfect
43 detection, enabling estimation of the sampling completeness of interaction networks grounded in
44 ecological mechanisms.

45 Imperfect detection is a pervasive feature of ecological sampling and has motivated a long history of
46 statistical approaches to account for it, e.g. rarefaction for species richness estimation (Sanders 1968,
47 Simberloff 1972). Explicitly accounting for imperfect detection has become common in modeling
48 occupancy (MacKenzie et al. 2002, Royle et al. 2005, Royle 2006), abundance (Royle 2004), ranges
49 (Guillera-Arroita 2017), and species richness (Dorazio and Royle 2005) with extensions to joint
50 modeling of co-occurrence (Pollock et al. 2014, Devarajan et al. 2020). Similarly, there has been
51 considerable work on sampling properties of interaction networks, primarily food-webs (Martinez et
52 al. 1999, McLeod et al. 2021). This work has motivated the use of rarefaction methods from species
53 richness estimation (Chacoff et al. 2012) to evaluate the completeness of network sampling,
54 quantifying the effect of underlying network topology on measurement bias (Aguilar et al. 2019),
55 consideration of the impacts of spatial and taxonomic biases (Poisot et al. 2021), and by excluding
56 biologically infeasible interactions from consideration (Jordano 2016a). Cirtwill et al. (2019)
57 introduced a framework describing the construction of empirical interaction networks accounting
58 for variability in realization and detection rates.

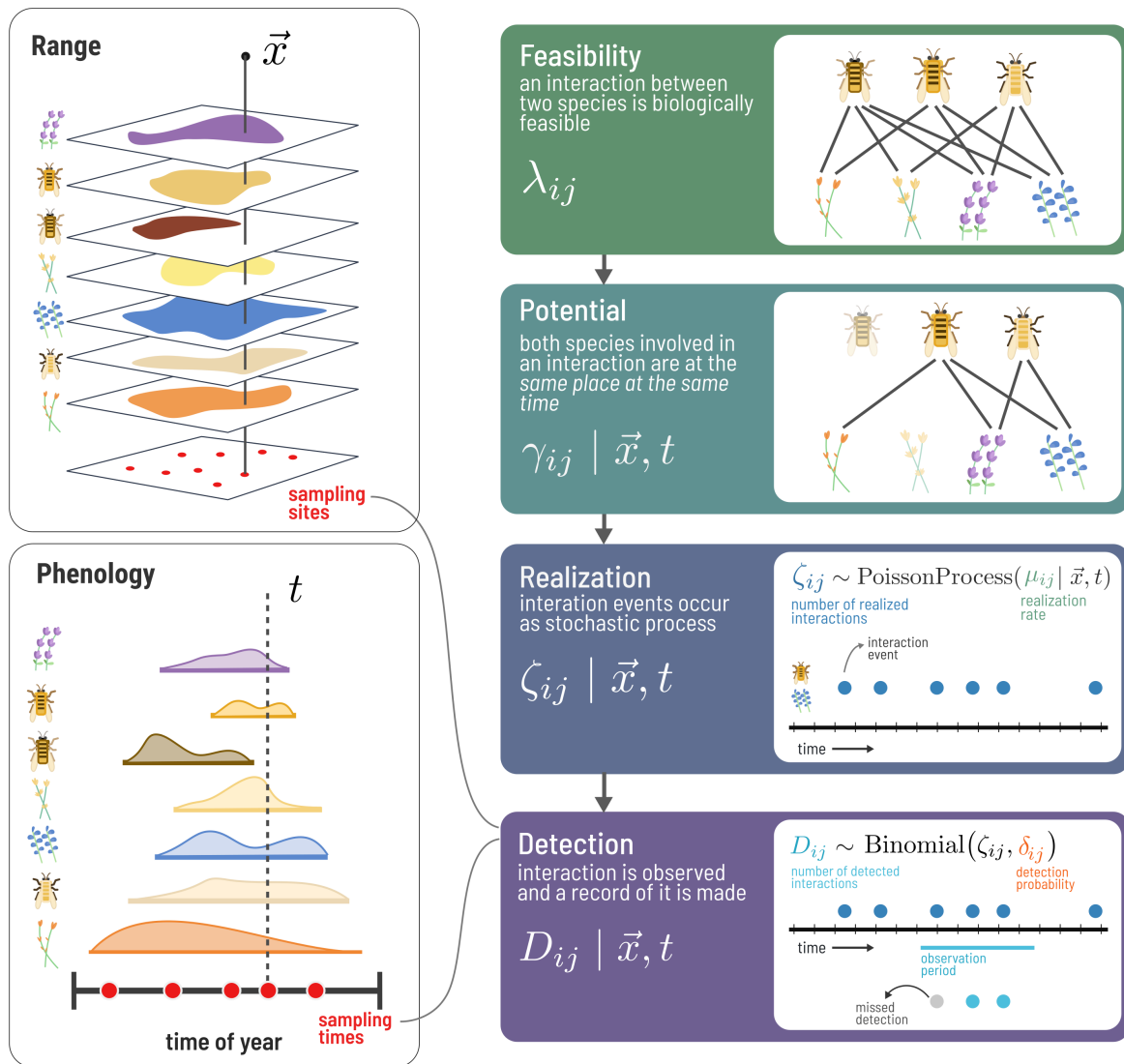
59 We extend the framework from Cirtwill et al. (2019) by developing a process-based model of
60 interaction realization and detection that explicitly accounts for spatiotemporal variation in species
61 occurrence and abundance, which intrinsically structures interactions across space and time (Poisot
62 et al. 2015). This framework links realization and detection rates to species abundance, moving
63 beyond rarefaction-based estimates of sampling completeness by linking interaction accumulation to
64 ecological mechanisms. We implement this framework in an open source software package,

65 SpeciesInteractionSamplers.jl. This approach allows researchers to both (1) estimate sampling
66 completeness under biologically realistic assumptions, and (2) evaluate the sampling design of
67 interaction monitoring programs.

68 **2 A Process-Based Framework for Spatiotemporal Species** 69 **Interaction Realization and Detection**

70 Quantifying the sampling completeness of species interaction networks is essential to assess the
71 limitations of inference made from interaction data, and to make grounded predictions of
72 interactions. To enable robust estimates of sampling completeness, we need to root this
73 methodology in the ecological processes that enable species interactions in order to ground these
74 estimates in ecological reality. We introduce a process-based model of the realization and detection
75 of species interactions that explicitly accounts for spatiotemporal variation in species presence and
76 abundance. [Cirtwill et al. \(2019\)](#) models how empirical species interaction networks are constructed
77 by having all pairwise species combinations move through a sequence of filters from all pairs of
78 species to those that are detected during data collection: (1) feasibility (an interaction is biologically
79 possible based on the traits of each species ([Banville et al. 2025](#))), (2) realization (a feasible
80 interaction actually happens), and (3) detection (the interaction is observed and recorded by an
81 observer).

82 We extend this framework in several ways: (1) By introducing a new filter, potential, which
83 disentangles co-occurrence from realization to account for spatiotemporal variation in abundance
84 and occurrence. Explicitly accounting for this variation is essential to account for the demographic
85 and biogeographic processes that structure interactions across space. The species interactions that
86 are realized at different locations and times is inherently structured by the distribution and
87 abundance of species across space, and separating co-occurrence from realization allows us to model
88 these processes independently, (2) by modeling the realization of interactions as a stochastic process
89 dependent on species abundances and/or traits, and (3) by explicitly modeling imperfect detection of
90 interactions by an observer.



91 **Figure 1:** A spatiotemporal framework for interaction detection. Building upon the feasibility-realization-detection
 92 framework from Cirtwill et al. (2019), we introduce a new filter that feasible interactions go through before they are
 93 detected – potential – which explicitly accounts for species co-occurrence.

94 2.1 Interaction Feasibility

95 The first filter on interactions across all pairs of species to those that are detected is interaction
 96 feasibility, where an interaction is feasible if both species involved have the biological capability to
 97 interact Cirtwill et al. (2019). We denote the feasibility of an interaction between species i and j as
 98 $\lambda_{ij} \in \{0, 1\}$

99 The feasibility of a given interaction is governed by numerous factors depending on the particular
 100 system and taxa of interest. These can be morphological traits (e.g. body-size in food webs (Cohen et
 101 al. 2003), bill length in hummingbird pollinated systems (Vizentin-Bugoni et al. 2014), or based in
 102 genetics (e.g. the protein structure of receptors in a virus and host (Diamond 2009)).

103 Although an interaction between two species may be feasible ($\lambda_{ij} = 1$), this does not necessarily
104 imply all individuals of each species can feasibly interact. Within-species variation in feasibility can
105 vary, for example due to phenotypic plasticity enabling an interaction between some members of
106 species and not others, or due to differences in morphology across life-stages.

107 **2.2 Interaction Potential**

108 Within [Cirtwill et al. \(2019\)](#)'s framework, both species co-occurrence and interaction are bundled
109 into the realization filter that describes if interactions are realized during a given sampling event or
110 not. We disentangle these two processes to make this framework spatiotemporally explicit by
111 introducing a new filter, interaction potential, between feasibility and realization (Figure 1), which is
112 dependent on the co-occurrence of both species involved in an interaction at a particular place x and
113 time t .

114 This separates the co-occurrence component of interactions from their stochastic realization,
115 enabling explicit modeling of the spatiotemporal heterogeneity in interaction networks due to
116 variation in species abundance and occurrence, which can then influence the rate of interaction
117 realization. We denote the occurrence of species i at location x and time t as $\gamma_i^{(x,t)}$, which is either a
118 binary variable indicating presence (i.e. $\gamma_i^{(x,t)} \in \{0, 1\}$), or a measure of relative species density (i.e.
119 $\gamma_i^{(x,t)}$ is between 0 and 1).

120 **2.3 Interaction Realization**

121 We introduce a family of process-based models of interaction realization. In the real world, species
122 interactions are not regular and deterministic, but sporadic and stochastic. Therefore, we model the
123 interaction realization as a Poisson process, where the number of events per unit of time is described
124 by a rate parameter μ , and during a single unit of time, the number of events that occur is
125 distributed as a $\text{Poisson}(\mu)$ distribution. We are then left with two separate challenges when
126 choosing how to define interaction rates: (1) defining the total number of expected number of
127 interactions across all interacting species per unit of time and (2) defining the rate of each particular
128 interaction.

129 To govern the expected total number of interactions, we introduce a “realization energy” parameter
130 ε , which governs the total number of expected interactions across all pairs of potentially interacting
131 species at a given site and/or time. We then define a set of models for determining per-interaction
132 rates that are (1) Abundance-based, (2) Trait-Matching based, and (3) Both Abundance and Trait-
133 Matching based.

134 **Abundance Based Realization**

135 The core idea of abundance-based realization is that more abundant species are more likely to
136 encounter each other in nature, and therefore the rate of interaction realization between two species
137 i and j is a function of each species' abundance (the mass action hypothesis; [Staniczenko et al.](#)
138 [\(2013\)](#)). We use this idea to describe a family of interaction realization models.

139 We start by defining a global distribution relative abundance \mathcal{R} that is pooled across all locations
140 and times. We denote the relative abundance of species i as R_i , and by definition

$$\sum_i R_i = 1$$

141 We then define the rate interaction $\mu_{ij}^{(x,t)}$ between species i and j at location x and time t as

$$\mu_{ij}^{(x,t)} = \frac{\varepsilon \cdot \lambda_{ij} \cdot f\left(r_i \gamma_i^{(x,t)}, r_j \gamma_j^{(x,t)}\right)}{\sum_{mn} \lambda_{mn} f\left(r_m \gamma_m^{(x,t)}, r_n \gamma_n^{(x,t)}\right)}$$

142 where $\gamma_i^{(x,t)}$ is the presence/abundance of species i at location x and time t , and f is a function for
143 combining abundances, e.g. arithmetic or geometric mean of abundances, the product of
144 abundances, or minimum/maximum abundance.

145 Note that the reason for normalization (the denominator in the above equation) is to ensure
146 $\sum_{ij} \mu_{ij}^{(x,t)} = 1$, meaning the expected number of realized interactions is controlled only by the
147 energy parameter, thereby decoupling parameters that control species-level occurrence and density
148 from the overall number of realized interactions per site/time.

149 **Trait-Matching Based Realization**

150 A second model of interaction rates relates interaction realization rates to species' traits. This
151 enables incorporating species "preferences" among potential interactions into interaction rates.

152 We consider each species having an arbitrary dimensional set of traits $z_i \in \mathbb{R}^N$, and we compute
153 species traits matching using the Euclidean distance $|z_i - z_j|$, and compute the contribution to
154 interaction rate using a kernel function k (e.g. Gaussian or exponential distance). The rate
155 interaction $\mu_{ij}^{(x,t)}$ between species i and j at location x and time t is then computed in a similar way
156 as before:

$$\mu_{ij}^{(x,t)} = \frac{\varepsilon \cdot \lambda_{ij} \cdot k(z_i, z_j)}{\sum_{mn} \lambda_{mn} k(z_m, z_n)}$$

157 **Abundance and Trait-Based Realization**

158 We can also combine abundance and trait-based realization by incorporating both species
159 abundances and the trait-kernel into the computation of $\mu_{ij}^{(x,t)}$ as

$$\mu_{ij}^{(x,t)} = \frac{\varepsilon \cdot \lambda_{ij} \cdot f\left(r_i \gamma_i^{(x,t)}, r_j \gamma_j^{(x,t)}\right) \cdot k(z_i, z_j)}{\sum_{mn} \lambda_{mn} f\left(r_m \gamma_m^{(x,t)}, r_n \gamma_n^{(x,t)}\right) \cdot k(z_m, z_n)}$$

160 2.4 Interaction Detection

161 Finally, to model detection, we introduce an abundance-mediated model of detection probability. We
 162 denote the probability of successful detection of an interaction between species i and j as δ_{ij} . We
 163 model species-level detection probability as $\delta_i = 1 - (1 - r_i)^\alpha$ where α is a scaling parameter that
 164 controls detectability, and as $\alpha \rightarrow 0$, the probability of detecting rare species approaches 0. We then
 165 treat the probability of detecting an interaction as function of each species' detection probabilities,
 166 i.e. $\delta_{ij} = f(\delta_i, \delta_j)$, where f is e.g. the arithmetic or geometric mean product or minimum/maximum
 167 abundance, mirroring how the abundance can be combined to compute realization rates.

168 The number of detected interactions between species i and j is then drawn from a binomial
 169 distribution as $D_{ij}^{(x,t)} \sim \text{Binomial}\left(\zeta_{ij}^{(x,t)}, \delta_{ij}\right)$, where $\zeta_{ij}^{(x,t)}$ is the number of realized interactions
 170 drawn from $\zeta_{ij}^{(x,t)} \sim \text{Poisson}\left(\mu_{ij}^{(x,t)}\right)$.

171 3 Case Studies

172 Here we demonstrate how this framework can be used to quantify the sampling completeness of an
 173 interaction network as a function of how many total (non-unique) interactions have been detected in
 174 a given dataset. We do this using a software package we developed, SpeciesInteractionSamplers.jl, in
 175 the Julia language, which implements this framework. SIS contains numerous methods for
 176 generating feasible networks, ranges, and phenologies, and a variety of methods for interaction
 177 realization and detection, including the abundance-based models described above. The full set of
 178 features is described in the documentation [here](#).

179 In these case studies, we explore how this relationship changes as a function of realization mode,
 180 detection, and spatial sampling effort. We measure sampling completeness using interaction
 181 accumulation curves, which measure the proportion of feasible interactions that have been detected
 182 as a function of the total number of (non-unique) interactions that have been detected.

183 3.1 Realization Rate

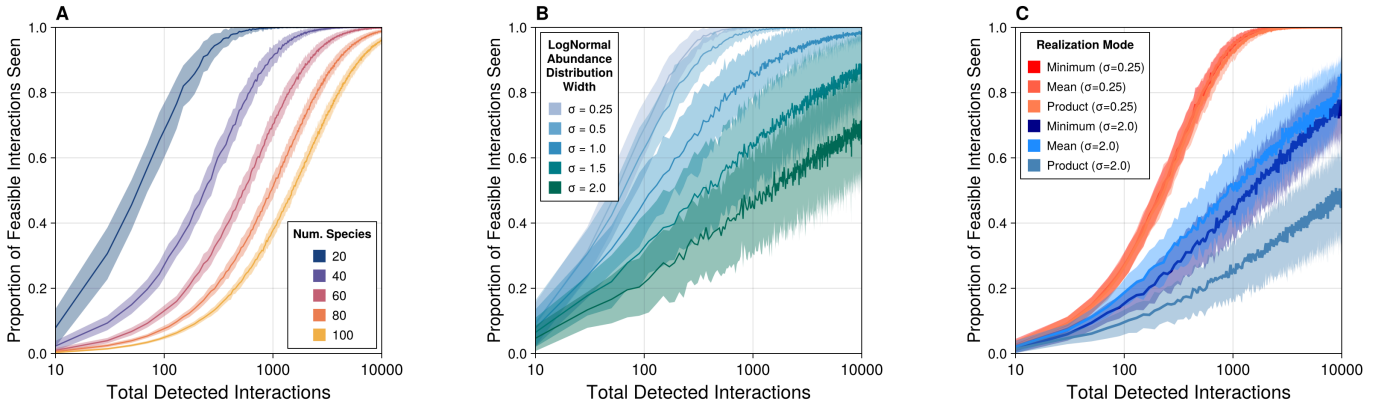
184 We first consider how the number of species, the shape of the species abundance distribution, and
 185 the relationship between abundance and realization rate affects interaction accumulation curves in
 186 networks without any spatial or temporal structure. All below results use the product of species
 187 abundances to parameterize realization rate, and the mean of species-level detectability ($\delta_i = 1 -$

188 $(1 - r_i)^\alpha$ with $\alpha = 20$) to parameterize the probability of interaction detection, unless one of these
189 factors is the variable of interest being varied.

190 Because the total number of detected interactions is not an input parameter to the framework, we
191 use an adaptive sampling scheme to generate interaction accumulation curves. Realization energy is
192 the parameter we have control over, but the distribution of total detected interactions for a given
193 energy value is a function of the models of realization and detection and their parameters. To get an
194 even sample across the number of total detected interactions, we first do a small “pilot” run across a
195 range of energy values with a small number of samples, and use linear regression to estimate the
196 relationship between realization energy and total detected interactions. This enables simulation of
197 interaction accumulation curves that are evenly spread across the number of total detected
198 interactions. Here, each pilot run consists of 25 replicates of generated interaction networks across
199 thirty energy values spread evenly between 0 and 50,000 to estimate the relationship between
200 energy and number of detected interactions. Then, bins of total detected interactions of size 20,
201 ranging from 0 to 10,000, are filled until 100 replicates are reached per bin.

202 Figure 2 contains simulations of food-web interaction accumulation curves under different numbers
203 of species, abundance distributions, and realization modes. All feasible interaction networks are
204 generated using the niche model of food webs (Williams and Martinez 2000) with connectance of 0.2.
205 In Figure 2(A) we consider different species pool sizes. Unsurprisingly, networks composed of more
206 species require more detected interactions to reach the same level of completeness. In Figure 2(B),
207 we look at how the shape of the species abundance distribution (SAD) impacts interaction
208 accumulation. We model the SAD as a LogNormal(σ) distribution (Preston 1948) with σ controlling
209 the width of the distribution. Low values of σ correspond to nearly uniform SADs, and high σ
210 corresponds to uneven distributions, with many individuals of common species and few individuals
211 of rare species. We find that the more even the distribution of abundances is, the more quickly the
212 sampling completeness of the network increases.

213 In Figure 2(C), we examine the impact of how abundances are combined to create realization rate in
214 networks with even ($\sigma = 0.2$) and uneven ($\sigma = 2.0$) log-normal abundance distributions. The impact
215 of the method for combining abundances used to compute realization rate is context-dependent:
216 when abundances are long-tailed, the way abundances are combined to compute realization rate
217 produces slower accumulation of unique detected interactions, as interactions involving very rare
218 species have far lower realization rate when the rate is scaled by multiplying relative abundances
219 than taking the mean. This extends to using the minimum of species abundance, which is slightly
220 slower to accumulate detected interactions than the mean. In contrast, when abundances across
221 species are even, there is little difference between product/mean/minimum modes.



222 **Figure 2:** (A) The interaction accumulation curve for different sized species pools (colors). (B) The interaction
 223 accumulation curve across log-normal abundance distributions with different variances (colors). (C) The interaction
 224 accumulation curve under even (red) and uneven (blue) species abundance distributions. Different shades indicate
 225 different methods of combining abundance when computing realization rate (mean, minimum, product).

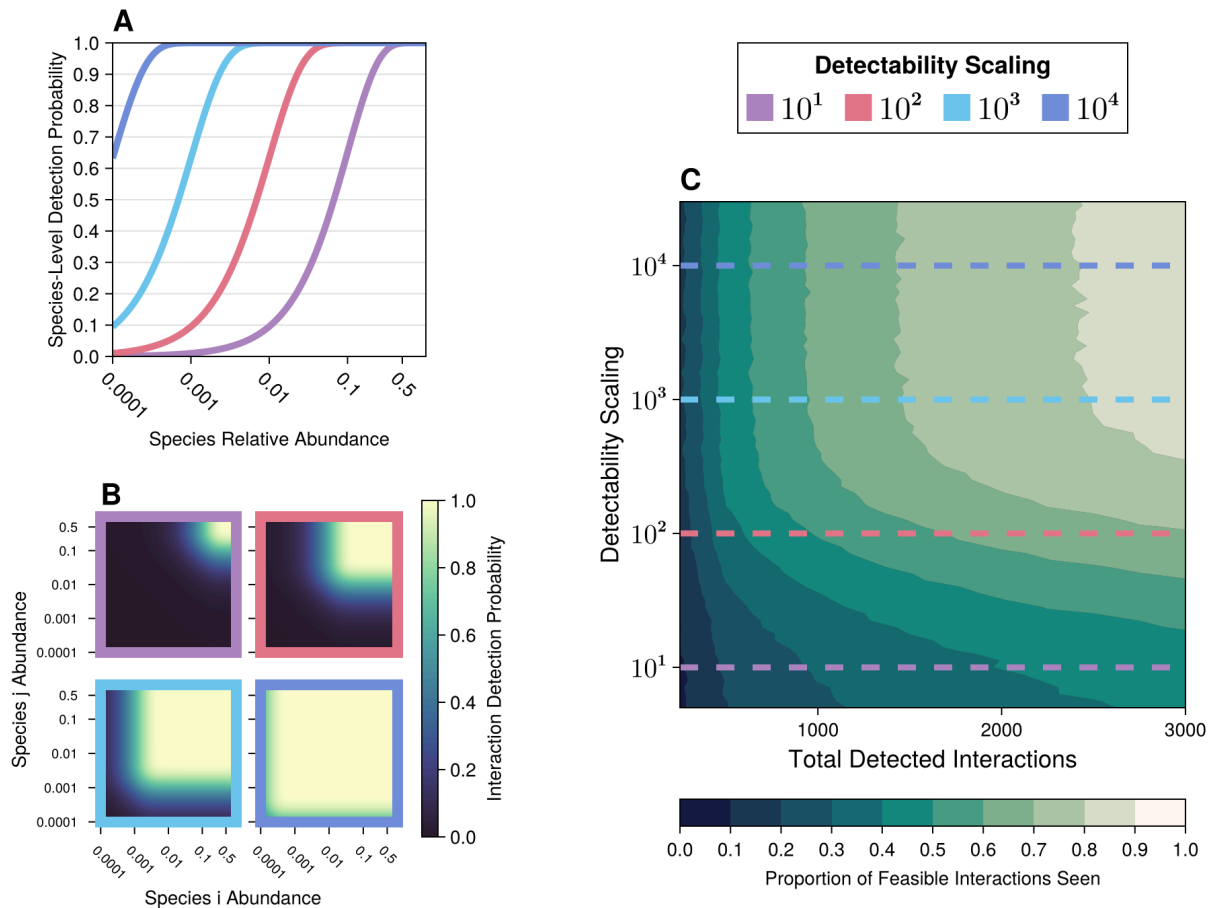
226 3.2 Detection

227 We now shift toward focusing on the impact of the interaction detection model on the interaction
 228 accumulation curve by adjusting the parameters of the abundance-dependent detection model. We
 229 adjust the adaptive sampling scheme used above to fit a unique linear model for each unique
 230 detectability scaling parameter to predict the average detected interactions per site as a function of
 231 the input energy. In practice, we found fitting a log-log regression, i.e.

$$\log(\text{energy}) \sim \log(\text{total detected})$$

232 produced a more even number of samples per bin.

233 In Figure 3(A), we see the species-level detection probability across different values of the scaling
 234 parameter α . The interaction detection rate, when being combined as the product of species-level
 235 detection, is shown for each combination of species relative abundance in Figure 3(B). Finally, the
 236 proportion of feasible interactions seen is shown as a function of both the total number of detected
 237 interactions and a gradient of the detectability scaling parameter in Figure 3(C). This emphasizes the
 238 importance of the detectability of interactions between rare species on the rate of interaction
 239 accumulation.



240 **Figure 3:** (A) The species-level detectability as a function of relative abundance (x-axis) under different detectability
 241 scaling parameters (colors). (B) The interaction detection probability across the relative-abundance of each involved
 242 species using the product mode of combining species-level scores. The color of each box corresponds to the
 243 detectability scaling parameter. (C) The proportion of feasible interactions that have been detected (colors) across a
 244 continuous gradient of the detectability scaling parameter (y-axis) and the total number of non-unique detected
 245 interactions (x-axis).

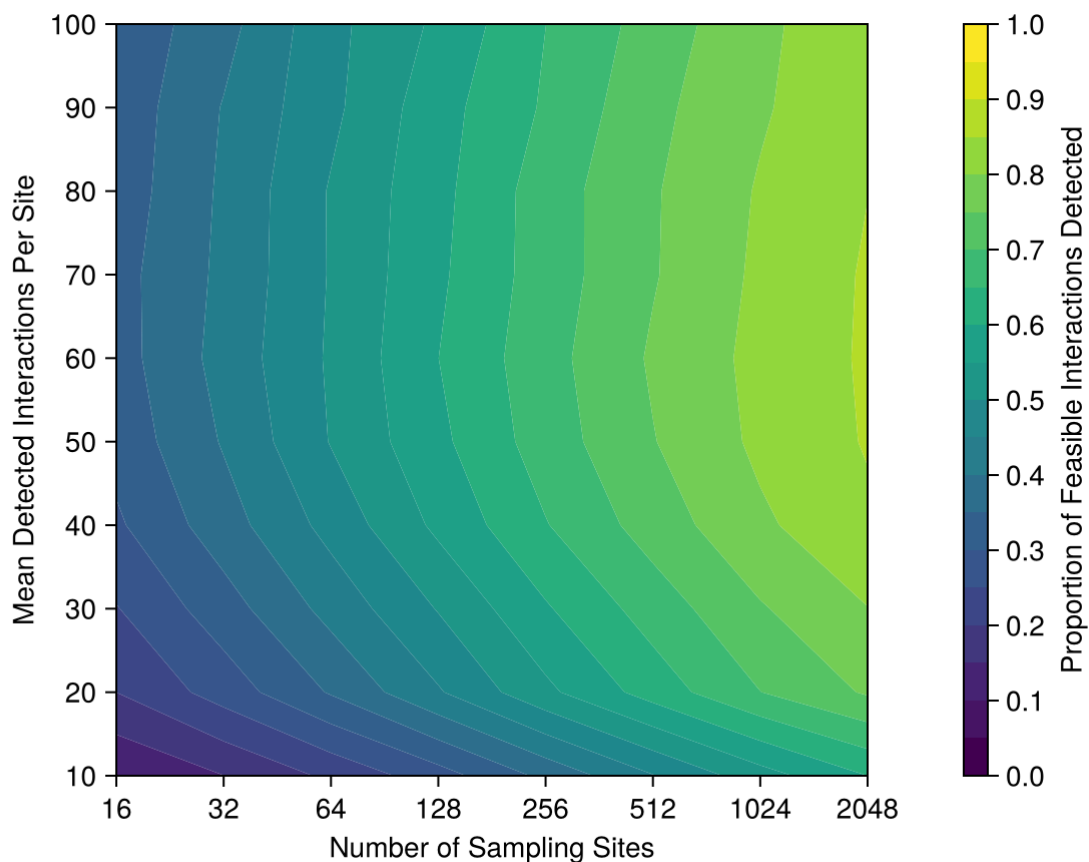
246 3.3 Spatial Coverage

247 Finally, we consider spatial variability in species occurrence. A practical challenge for sampling
 248 species interactions given the spatial variation in species ranges is determining how many sampling
 249 locations are needed to get a complete picture of the regional metaweb.

250 We generate 30 species food-webs using the niche model (Williams and Martinez 2000), with a
 251 connectance of 0.2. Ranges were generated using the Midpoint-Displacement algorithm with an
 252 autocorrelation parameter of 0.85, where the prevalence of each species is drawn from a
 253 Beta(10, 10) distribution (meaning range sizes are highly concentrated around 50% of the total
 254 extent). We simulate spatial networks with 64 replicates per unique number of sampling sites and
 255 energy values ranging for 100 to 1000 (in intervals of 100), governing the expected number of
 256 interactions realized per sampling site. For simplicity, we use a homogenous distribution of energy

257 across space, so the expected number of realized interactions is the same across all sites. Similar to
258 the previous case study, we adjust the adaptive sampling scheme by fitting a unique linear model for
259 each number of sampling sites to predict the average detected interactions per site as a function of
260 the input energy.

261 In Figure 4, we show the proportion of total feasible interactions in the metaweb detected across the
262 number of sampled sites and the average number of (non-unique) detected interactions per sampling
263 site. This shows that beyond a given level of sampling effort at each site (an average of 20
264 interactions detected per site), the primary driver of interaction accumulation is the total number of
265 sites, not the effort at each site.



266 **Figure 4:** The proportion of feasible interactions that have been detected (colors) as a function of the number of
267 sampling sites (x-axis; log scale) and the mean number of interactions detected at each site (y-axis).

268 **4 Discussion**

269 Species interactions underpin ecosystem function, but still remain a massive gap in our
270 understanding of ecology (Hortal et al. 2015) due to the intrinsic difficulty imposed by interaction
271 sampling (Jordano 2016a). Here, we have introduced a framework to calculate the size of this
272 shortfall in empirical data by extending the framework for interaction detection from Cirtwill et al.

273 (2019) to a process-based model of interaction realization and detection. This enables simulation of
274 interaction accumulation curves in spatiotemporally variable networks, where realization and
275 detection is a function of species abundances, to estimate the sampling completeness of networks as
276 a function of effort. We provide an associated software package, SpeciesInteractionSamplers.jl,
277 which enables generation of feasible interaction networks, species ranges, phenologies, and
278 abundances using a variety of models, and a variety of models of interaction realization and
279 detection.

280 These tools provide a method to estimate the number of “missing” interactions in sampled networks
281 as a function of sampling effort, and provide a sandbox for testing different strategies for designing
282 monitoring schemes to most effectively sample interactions in spatiotemporally variable networks.
283 This work has practical implications for the design of surveys of species interactions. First, the
284 structure of species co-occurrence must be considered when sampling interactions. This is impacted
285 by the goal of sampling: if the aim is targeting interactions whose feasibility we are most uncertain
286 about, sampling design should select locations that maximize the chance of observing species co-
287 occurrence. If instead the goal is broad-scale characterization of the ecological network across a
288 large region, the goal should be to target sampling to be representative of the co-occurrence
289 structure across space. This framework and software can then be used to test the efficacy of different
290 monitoring design programs under known “ground-truth” scenarios of interaction network structure
291 and spatiotemporal distribution.

292 Second, given the increased interest in using models to predict feasible but unobserved interactions
293 between species based on traits (Gravel et al. 2013, Strydom et al. 2021, Caron et al. 2022), these
294 methods provide a useful tool for estimating the number of interactions “missing” from the sampled
295 data as a function of sampling effort and the spatiotemporal distribution of species. Having even a
296 rough estimate of true class balance (the ratio of how many positives to negatives are expected in
297 the true data) can be useful in training models to predict interactions (Poisot 2022).

298 Further, explicitly accounting for imperfect detection in occurrence and abundance modeling is
299 increasingly common (Royle et al. 2005). Although the use of predictive models has seen increased
300 use for imputing feasible interactions (Stock et al. 2017, Young et al. 2021), explicitly accounting for
301 detection error is not yet commonly adopted in these methods. The process-based models
302 introduced here provide a basis for incorporating the impact of abundance on interaction realization
303 and detection, and could be introduced into Bayesian models of interaction count data like presented
304 in Becker et al. (2022).

305 Finally, the consequences of sampling completeness of species interaction data can impact our
306 understanding of the impact of species interaction network structure on dynamics. For example,
307 inferring the dynamic stability of a network could be prone to error if the observed network is not
308 sampled “enough”. Song et al. (2022) show that the stability of sampled subnetworks can be used to

309 infer the stability of the overall metaweb beyond a threshold of samples. Future work could focus on
310 how robust this result is when species interaction coefficients are inferred from networks sampled
311 with realization and detection rates influenced by species abundance. Further, predictions about the
312 consequences of network rewiring (Thompson and Gonzalez 2017) due to range shifts in response to
313 climate change could be error-prone without accounting for interactions that have not been
314 observed but that still may become climatically infeasible.

315 A better understanding of sampling effects on the construction of species interaction networks is a
316 necessity to have a statistically robust estimate of the current state and change over time of species
317 interactions. This work provides a process-based framework for simulating the rate of interaction
318 accumulation when sampling, while accounting for spatiotemporal variation in interaction networks
319 (Poisot et al. 2015) and the effects of abundance on interaction realization and detection. This
320 provides a necessary step forward for developing a theory of interaction monitoring to improve our
321 understanding of species interaction networks and how they are changing.

322 **Code and Data Availability:** The code for SpeciesInteractionSamplers.jl is available on Github
323 [here](#).

324 **Acknowledgements:** MDC is funded by an IVADO Postdoctoral Fellowship. TP is funded by an
325 NSERC Discovery grant, a Discovery Acceleration Supplement grant, and a Wellcome Trust grant
326 (223764/Z/21/Z). AG and MDC were supported by the Liber Ero Chair in Conservation.

327 **References**

- 328 Aguiar MAM de, Newman EA, Pires MM, et al (2019) Revealing Biases in the Sampling of Ecological
329 Interaction Networks. *PeerJ* 7:e7566. <https://doi.org/10.7717/peerj.7566>
- 330 Banville F, Strydom T, Blyth PSA, et al (2025) Deciphering Probabilistic Species Interaction
331 Networks. *Ecology Letters* 28:e70161. <https://doi.org/10.1111/ele.70161>
- 332 Bartley TJ, McCann KS, Bieg C, et al (2019) Food Web Rewiring in a Changing World. *Nature*
333 *Ecology & Evolution* 3:345–354. <https://doi.org/10.1038/s41559-018-0772-3>
- 334 Becker DJ, Albery GF, Sjodin AR, et al (2022) Optimising Predictive Models to Prioritise Viral
335 Discovery in Zoonotic Reservoirs. *The Lancet Microbe* 3:e625–e637. [https://doi.org/10.1016/S](https://doi.org/10.1016/S2666-5247(21)00245-7)
336 [2666-5247\(21\)00245-7](https://doi.org/10.1016/S2666-5247(21)00245-7)
- 337 Carlson CJ, Albery GF, Merow C, et al (2022) Climate Change Increases Cross-Species Viral
338 Transmission Risk. *Nature* 607:555–562. <https://doi.org/10.1038/s41586-022-04788-w>
- 339 Caron D, Maiorano L, Thuiller W, Pollock LJ (2022) Addressing the Eltonian Shortfall with Trait-
340 Based Interaction Models. *Ecology Letters* 25:889–899. <https://doi.org/10.1111/ele.13966>
- 341 Chacoff NP, Vázquez DP, Lomáscolo SB, et al (2012) Evaluating Sampling Completeness in a Desert
342 Plant–Pollinator Network. *Journal of Animal Ecology* 81:190–200. [https://doi.org/10.1111/j.1365-](https://doi.org/10.1111/j.1365-2656.2011.01883.x)
343 [2656.2011.01883.x](https://doi.org/10.1111/j.1365-2656.2011.01883.x)
- 344 Cirtwill AR, Eklöf A, Roslin T, et al (2019) A Quantitative Framework for Investigating the Reliability
345 of Empirical Network Construction. *Methods in Ecology and Evolution* 10:902–911. [https://doi.](https://doi.org/10.1111/2041-210X.13180)
346 [org/10.1111/2041-210X.13180](https://doi.org/10.1111/2041-210X.13180)
- 347 Cohen JE, Jonsson T, Carpenter SR (2003) Ecological Community Description Using the Food Web,
348 Species Abundance, and Body Size. *Proceedings of the National Academy of Sciences* 100:1781–
349 1786. <https://doi.org/10.1073/pnas.232715699>
- 350 Devarajan K, Morelli TL, Tenan S (2020) Multi-Species Occupancy Models: Review, Roadmap, and
351 Recommendations. *Ecography* 43:1612–1624. <https://doi.org/10.1111/ecog.04957>
- 352 Diamond MS (2009) Virus and Host Determinants of West Nile Virus Pathogenesis. *PLOS Pathogens*
353 5:e1000452. <https://doi.org/10.1371/journal.ppat.1000452>
- 354 Dorazio RM, Royle JA (2005) Estimating Size and Composition of Biological Communities by
355 Modeling the Occurrence of Species. *Journal of the American Statistical Association* 100:389–398.
356 <https://doi.org/10.1198/016214505000000015>

357 Gravel D, Poisot T, Albouy C, et al (2013) Inferring Food Web Structure from Predator–Prey Body
358 Size Relationships. *Methods in Ecology and Evolution* 4:1083–1090. [https://doi.org/10.1111/2041-](https://doi.org/10.1111/2041-210X.12103)
359 210X.12103

360 Guillera-Aroita G (2017) Modelling of Species Distributions, Range Dynamics and Communities
361 under Imperfect Detection: Advances, Challenges and Opportunities. *Ecography* 40:281–295.
362 <https://doi.org/10.1111/ecog.02445>

363 Hortal J, De Bello F, Diniz-Filho JAF, et al (2015) Seven Shortfalls That Beset Large-Scale Knowledge
364 of Biodiversity. *Annual Review of Ecology, Evolution, and Systematics* 46:523–549. [https://doi.](https://doi.org/10.1146/annurev-ecolsys-112414-054400)
365 [org/10.1146/annurev-ecolsys-112414-054400](https://doi.org/10.1146/annurev-ecolsys-112414-054400)

366 Jordano P (2016b) Chasing Ecological Interactions. *PLOS Biology* 14:e1002559. [https://doi.org/10.](https://doi.org/10.1371/journal.pbio.1002559)
367 [1371/journal.pbio.1002559](https://doi.org/10.1371/journal.pbio.1002559)

368 Jordano P (2016a) Sampling Networks of Ecological Interactions. *Functional Ecology* 30:1883–1893.
369 <https://doi.org/10.1111/1365-2435.12763>

370 MacKenzie DI, Nichols JD, Lachman GB, et al (2002) Estimating Site Occupancy Rates When
371 Detection Probabilities Are Less Than One. *Ecology* 83:2248–2255. [https://doi.org/10.1890/0012-](https://doi.org/10.1890/0012-9658(2002)083[2248:ESORWD]2.0.CO;2)
372 [9658\(2002\)083\[2248:ESORWD\]2.0.CO;2](https://doi.org/10.1890/0012-9658(2002)083[2248:ESORWD]2.0.CO;2)

373 Makiola A, Compson ZG, Baird DJ, et al (2020) Key Questions for Next-Generation Biomonitoring.
374 *Frontiers in Environmental Science* 7:

375 Martinez ND, Hawkins BA, Dawah HA, Feifarek BP (1999) Effects of Sampling Effort on
376 Characterization of Food-Web Structure. *Ecology* 80:1044–1055. [https://doi.org/10.1890/0012-9658](https://doi.org/10.1890/0012-9658(1999)080[1044:EOSEOC]2.0.CO;2)
377 [\(1999\)080\[1044:EOSEOC\]2.0.CO;2](https://doi.org/10.1890/0012-9658(1999)080[1044:EOSEOC]2.0.CO;2)

378 McLeod A, Leroux SJ, Gravel D, et al (2021) Sampling and Asymptotic Network Properties of Spatial
379 Multi-Trophic Networks. *Oikos* 130:2250–2259. <https://doi.org/10.1111/oik.08650>

380 Poisot T (2022) Guidelines for the Prediction of Species Interactions through Binary Classification

381 Poisot T, Bergeron G, Cazelles K, et al (2021) Global Knowledge Gaps in Species Interaction
382 Networks Data. *Journal of Biogeography* 48:1552–1563. <https://doi.org/10.1111/jbi.14127>

383 Poisot T, Stouffer DB, Gravel D (2015) Beyond Species: Why Ecological Interaction Networks Vary
384 through Space and Time. *Oikos* 124:243–251. <https://doi.org/10.1111/oik.01719>

385 Pollock LJ, Tingley R, Morris WK, et al (2014) Understanding Co-occurrence by Modelling Species
386 Simultaneously with a Joint Species Distribution Model (\textsc{JSDM}). *Methods in Ecology*
387 *and Evolution* 5:397–406. <https://doi.org/10.1111/2041-210X.12180>

388 Preston FW (1948) The Commonness, And Rarity, of Species. *Ecology* 29:254–283. <https://doi.org/10.2307/1930989>

390 Royle JA (2006) Site Occupancy Models with Heterogeneous Detection Probabilities. *Biometrics*
391 62:97–102. <https://doi.org/10.1111/j.1541-0420.2005.00439.x>

392 Royle JA (2004) N -Mixture Models for Estimating Population Size from Spatially Replicated
393 Counts. *Biometrics* 60:108–115. <https://doi.org/10.1111/j.0006-341X.2004.00142.x>

394 Royle JA, Nichols JD, Kéry M (2005) Modelling Occurrence and Abundance of Species When
395 Detection Is Imperfect. *Oikos* 110:353–359. <https://doi.org/10.1111/j.0030-1299.2005.13534.x>

396 Sanders HL (1968) Marine Benthic Diversity: A Comparative Study. *The American Naturalist*
397 102:243–282. <https://doi.org/10.1086/282541>

398 Simberloff D (1972) Properties of the Rarefaction Diversity Measurement. *The American Naturalist*
399 106:414–418

400 Song C, Simmons BI, Fortin M-J, et al (2022) Rapid Monitoring for Ecological Persistence.
401 2022.07.02.498308

402 Staniczenko PPA, Kopp JC, Allesina S (2013) The Ghost of Nestedness in Ecological Networks.
403 *Nature Communications* 4:1391. <https://doi.org/10.1038/ncomms2422>

404 Stock M, Poisot T, Waegeman W, De Baets B (2017) Linear Filtering Reveals False Negatives in
405 Species Interaction Data. *Scientific Reports* 7:45908. <https://doi.org/10.1038/srep45908>

406 Strydom T, Catchen MD, Banville F, et al (2021) A Roadmap towards Predicting Species Interaction
407 Networks (across Space and Time). *Philosophical Transactions of the Royal Society B: Biological*
408 *Sciences* 376:20210063. <https://doi.org/10.1098/rstb.2021.0063>

409 Terry JCD, Lewis OT (2020) Finding Missing Links in Interaction Networks. *Ecology* 101:e3047.
410 <https://doi.org/10.1002/ecy.3047>

411 Thompson PL, Gonzalez A (2017) Dispersal Governs the Reorganization of Ecological Networks
412 under Environmental Change. *Nature Ecology & Evolution* 1:1–8. [https://doi.org/10.1038/s41559-
413 017-0162](https://doi.org/10.1038/s41559-017-0162)

414 Vizontin-Bugoni J, Maruyama PK, Sazima M (2014) Processes Entangling Interactions in
415 Communities: Forbidden Links Are More Important than Abundance in a Hummingbird–Plant
416 Network. *Proceedings of the Royal Society B: Biological Sciences* 281:20132397. [https://doi.org/
417 10.1098/rspb.2013.2397](https://doi.org/10.1098/rspb.2013.2397)

418 Williams RJ, Martinez ND (2000) Simple Rules Yield Complex Food Webs. *Nature* 404:180–183.

419 <https://doi.org/10.1038/35004572>

420 Young J-G, Valdovinos FS, Newman MEJ (2021) Reconstruction of Plant–Pollinator Networks from

421 Observational Data. *Nature Communications* 12:3911. <https://doi.org/10.1038/s41467-021-24149-x>